5. Jun, L. *et al. Phys. Rev. D* **44,** 2611–2613 (1991).
6. Kuusela, T. *Phys. Rev. D* **43,** 2041–2043 (1991).
7. Kuusela, T. *Gen. Relativ. Grav.* **24,** 543–551 (1992).
8. Mishra, D. C. & Rao, M. B. S. *Curr. Sci.* **72,** 782–783 (1997).
9. Turneaure, J. P., Will, C. M., Farrell, B. F., Mattison, E. M. & Vessot, R. F. C. *Phys. Rev. D* **27,** 1705–1714 (1983).
10. Prestage, J. D., Tjoelker, R. L. & Maleki, L. *Phys. Rev. Lett.* **74,** 3511–3514 (1995).

Colloidal particles

Origin of anomalous multibody interactions

In a numerical study, Bowen and Sharif[1] purported to capture attractive interactions between like-charged colloidal particles by solving the nonlinear Poisson–Boltzmann equation around two particles in a pore. We are unable to replicate their results, in accord with recent proofs[2,3] showing that this equation cannot produce attractions between like-charged particles. Our calculations reveal only repulsive interactions between confined particles, indicating that the cause for anomalous colloidal multibody interactions is still unknown.

Colloidal interactions are critical to a variety of processes, including bacterial adhesion[4], the flow of colloidal dispersions[5], and the self-assembly of nanoparticles to form optoelectronic devices[6]. Electrostatic interactions between colloidal particles are fairly well described by the Derjaguin–Landau–Vervey–Overbeek (DLVO) theory[7,8]. However, direct measurement has revealed qualitative departures from this theory in multibody, low-salt situations[9,10]. Theoretical work[11–15] has tried to describe the attractions between like-charged colloidal particles.

Like Bowen and Sharif, we solved the nonlinear Poisson–Boltzmann equation in an axisymmetric geometry. We performed finite-element simulations using FIDAP software with successive grid refinement to check the convergence of our results. A fine grid is needed to obtain accurate results, and integrating the stress tensor over the midplane between particles and over a parallel plane far from the particles allows us to obtain faster convergence than was achieved by Bowen and Sharif, although we checked our results using their technique of integrating over the sphere surface. Our typical grid contains 100,000 nodes, including 220 on the surface of the sphere, twice as many as Bowen and Sharif. We also used regular grid spacings near the important boundaries to minimize numerical noise.

We found that colloidal particles in a pore are repulsive at all distances — indeed, the pore has only a small mitigating effect on the repulsions relative to isolated particles (Fig. 1). Using the same parameters as Bowen and Sharif, the gap between the particle surface and the pore surface is approximately eight Debye lengths, so only a small perturbative effect was expected. (The Debye length, κ^{-1}, is inversely proportional to the square root of the salt concentration, and represents the decay length of screened electrostatic interactions.)

Multibody effects are known to mitigate repulsions between cylinders in planar slits[11], but significant effects are not seen until the confining walls are within the range of 1–2 Debye lengths. Increasing the confinement of the pore geometry by reducing the pore wall–particle gap to one Debye length results in significantly smaller repulsive interactions than for isolated spheres (Fig. 1), but there are still no attractions.

Our results are in keeping with proofs[2,3] that the nonlinear Poisson–Boltzmann equation cannot produce attractive forces for the conditions simulated here and in general for confined or unconfined colloids in a system with mirror symmetry and overall electroneutrality. Together with these proofs, our results indicate that there may be an insidious error in the computations of Bowen and Sharif. In addition, the proofs[2,3] show that solutions of the mean-field nonlinear Poisson–Boltzmann equation cannot explain electrostatic interactions between like-charged colloidal particles[9], so new physical theories need to be developed.

Jeffrey J. Gray, Benny Chiang, Roger T. Bonnecaze
Department of Chemical Engineering, University of Texas at Austin, Austin, Texas 78712-1062, USA

1. Bowen, W. R. & Sharif, A. O. *Nature* **393,** 663–665 (1998); correction *Nature* **402,** 841 (1999).
2. Neu, J. C. *Phys. Rev. Lett.* **82,** 1072–1074 (1999).
3. Sader, J. E. & Chan, D. Y. C. *J. Colloid Interface Sci.* **213,** 268–269 (1999).
4. Razatos, A. P., Ong, Y. L., Sharma, M. M. & Georgiou, G. *Proc. Natl Acad. Sci. USA* **95,** 11059–11064 (1998).
5. Chen, L.-B., Ackerson, B. J. & Zukoski, C. F. *J. Rheol.* **38,** 193–216 (1994).
6. Joannopoulos, J. D., Villeneuve, P. R. & Fan, S. *Nature* **386,** 143–149 (1997).
7. Derjaguin, B. V. & Landau, L. *Acta Physiochim.* **14,** 633–662 (1941).
8. Verwey, E. J. W. & Overbeek, J. T. G. *Theory of the Stability of Lyophobic Colloids: The Interaction of Sol Particles Having an Electric Double Layer* (Elsevier, New York, 1948).
9. Crocker, J. C. & Grier, D. G. *Phys. Rev. Lett.* **77,** 1897–1900 (1996).
10. Larsen, A. E. & Grier, D. G. *Nature* **385,** 230–233 (1997).
11. Ospeck, M. & Fraden, S. *J. Chem. Phys.* **109,** 9166–9171 (1998).
12. Kwon, G. W., Won, Y. S. & Yoon, B. J. *J. Colloid Interface Sci.* **205,** 423–432 (1998).
13. Stevens, M. J., Falk, M. L. & Robbins, M. O. *J. Chem. Phys.* **104,** 5209–5219 (1996).
14. Tehver, R., Ancilotto, F., Toigo, F., Koplik, J. & Banavar, J. R. *Phys. Rev. E* **59,** R1335–R1338 (1999).
15. Goulding, D. & Hansen, J.-P. *Europhys. Lett.* **46,** 407–413 (1999).

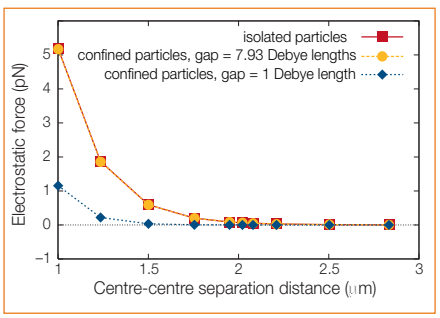

Figure 1 Plot of electrostatic force against distance between particles. Particles are either isolated, confined in a pore of radius 9.12 κ^{-1}, or confined in a pore of radius 2.185 κ^{-1}. For all simulations, the zeta potentials on the pore wall and on the surfaces of the particles are 128.5 and 77.1 mV, respectively, and $\kappa a = 1.185$, where the particle radius $a = 325$ nm. The salt is monovalent, the temperature is 298 K, and the relative permittivity is 78. Parameter values are the same as in ref. 1.

corrections

Hiding messages in DNA microdots

C. Taylor Clelland, V. Risca, C. Bancroft
Nature **399,** 533–534 (1999)

In line 16 of the second paragraph, "three-million-fold" should be replaced by "thirty-million-fold". This correction strengthens our original conclusions. In addition, some of the information in Fig. 1b was either missing or incorrect. The amended figure is shown here.

b

Encryption key

A=CGA	K=AAG	U=CTG	0=ACT
B=CCA	L=TGC	V=CCT	1=ACC
C=GTT	M=TCC	W=CCG	2=TAG
D=TTG	N=TCT	X=CTA	3=GCA
E=GGC	O=GGA	Y=AAA	4=GAG
F=GGT	P=GTG	Z=CTT	5=AGA
G=TTT	Q=AAC	=ATA	6=TTA
H=CGC	R=TCA	,=TCG	7=ACA
I=ATG	S=ACG	.=GAT	8=AGG
J=AGT	T=TTC	:=GCT	9=GCG

Ageing, fitness and neurocognitive function

A. F. Kramer *et al.*
Nature **400,** 418–419 (1999)

The key to Fig. 1b contained two errors: the second set of (dark-blue) bars represents the "incompatible pre-exercise" responses, and the third set of (light-brown) bars represents the "compatible post-exercise responses".

Dichromatism in macaque monkeys

A. Onishi *et al.*
Nature **402,** 139–140 (1999)

The eighth name in the list of authors, Hidehiko Komatsu, was spelt incorrectly. In the reference list, the first author of ref. 12, Jørgensen, A. L., was also spelt incorrectly.

Parasitoid behaviour and *Bt* plants

T. H. Schuler, R. P. J. Potting, I. Denholm, G. M. Poppy
Nature **400,** 825–826 (1999)

Figure 1b was incorrectly labelled: the bars on both sides should have read "*Bt*-resistant hosts".

brief communications is intended to provide a forum for both brief, topical reports of general scientific interest and technical discussion of recently published material of particular interest to non-specialist readers. Priority will be given to contributions that have fewer than 500 words, 10 references and only one figure. Detailed guidelines are available on *Nature*'s website (www.nature.com) or on request from **nature@nature.com**

Hiding messages in DNA microdots

The microdot is a means of concealing messages (steganography)[1] that was developed by Professor Zapp and used by German spies in the Second World War to transmit secret information[2]. A microdot ("the enemy's masterpiece of espionage"[2]) was a greatly reduced photograph of a typewritten page that was pasted over a full stop in an innocuous letter[2]. We have taken the microdot a step further and developed a DNA-based, doubly steganographic technique for sending secret messages. A DNA-encoded message is first camouflaged within the enormous complexity of human genomic DNA and then further concealed by confining this sample to a microdot.

A prototypical 'secret message' DNA strand contains an encoded message flanked by polymerase chain reaction (PCR) primer sequences (Fig. 1a). Encryption is not of primary importance in steganography, so we can use a simple substitution cipher[1] to encode characters in DNA triplets (Fig. 1b). Because the human genome contains about 3×10^9 nucleotide pairs, fragmented and denatured human DNA provides a very complex background for concealing secret-message DNA. For example, a secret message 100 nucleotides long added to treated human DNA at one copy per haploid genome would be hidden in a roughly three-million-fold excess of physically similar DNA strands. Confining such a sample to a microdot might then allow even the medium containing the message to be concealed from an adversary. However, the intended recipient, knowing both the secret-message DNA PCR primer sequences and the encryption key, could readily amplify the DNA and then read and decode the message.

Even if an adversary somehow detected such a microdot, it would still prove extremely difficult to read the message without knowing the specific primer sequences. For example, if 20-base random primers were used to amplify the DNA, separate amplifications with more than 10^{20} different primer pairs would be required, even allowing three mismatches per primer, followed by analysis of any PCR products obtained. Similar considerations apply to attempts to shotgun-clone the DNA sample and analyse the resultant clones. So even if the same primer pair were used on several occasions, an enemy trying to detect the primer sequences would face an extremely difficult experimental barrier. Further mathematical and biochemical analysis would therefore be expected to prove that the primer pairs used in this technique are not analogous to a classic, single-use, cryptographical "one-time pad"[1].

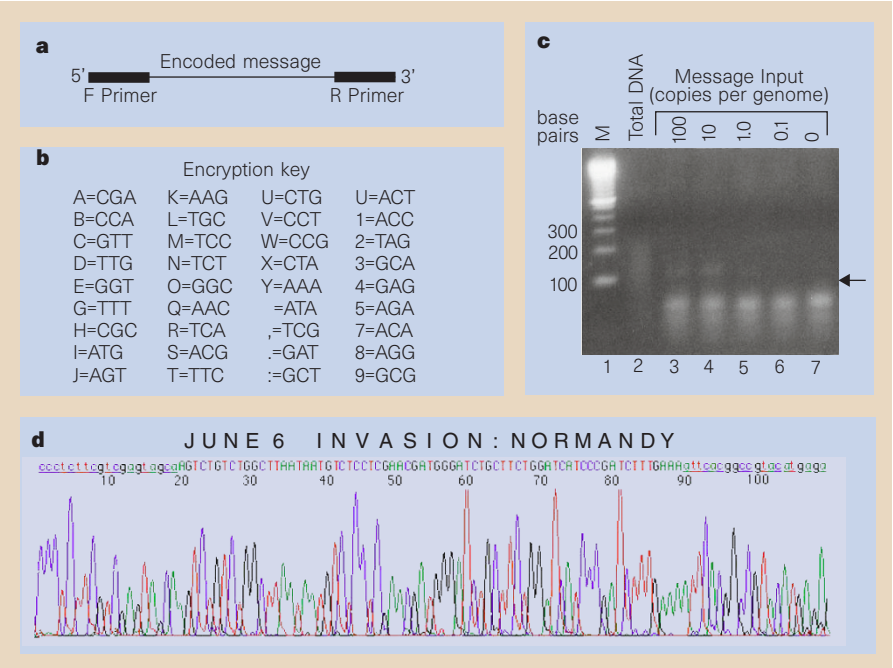

Figure 1 Genomic steganography. **a,** Structure of a prototypical secret-message DNA strand. F, forward; R, reverse. **b,** Key used to encode a message in DNA. **c,** Gel analysis of products obtained by PCR amplification with specific primers of microdots containing secret-message DNA strands hidden in a background of sonicated, denatured human genomic DNA. Message input in copies per human haploid genome is indicated, where 1.0 corresponds to 0.41 femtograms of secret-message DNA in 11 nanograms of human DNA. Lane 2 contains a message input of 100 (20-fold more total DNA than the microdots) and was not PCR amplified. M, 100-base-pair size markers. The gel was stained with ethidium bromide. The arrow indicates the PCR product seen in some lanes, below which primer–dimer bands can be seen. **d,** Sequence of the cloned product of PCR amplification, and the result of using the encryption key to decode the message. The DNA sequence determined for the encoded message is shown; the flanking primer sequences are in lower case. For details of the experimental methodology, see Supplementary Information.

Attempts by an adversary to use a subtraction technique to detect the secret-message DNA concealed within human DNA could be blocked by using a random mixture of genomic DNAs from different organisms as background. The intended recipient could still use the same procedures to amplify and read the secret-message DNA, even if ignorant of the random mixture composition, and even if the primers artefactually amplified a limited number of genomic sequences, because the encryption key would reveal which PCR product encodes a sensible message. This technique would also allow a single or duplicate microdots to be used to send individual secret messages to each of several intended recipients, each of whom would use a unique set of primers to amplify only his or her intended message.

To investigate the feasibility of this scheme, we synthesized a secret-message DNA oligodeoxynucleotide containing an encoded message 69 nucleotides long flanked by forward and reverse PCR primers, each 20 nucleotides long. We prepared concealing DNA that is physically similar to the secret-message DNA by sonicating human DNA to roughly 50 to 150 nucleotide pairs (average size) and denaturing it. We pipetted 6 μl of each solution containing 225 ng of treated human DNA, plus various amounts of added secret-message DNA, over a 16-point full stop printed on filter paper; it finally occupied an area about 20 times the size of the full stop. Excision of the printed full stops, each containing about 10 ng of DNA and with a cross-section that was about 75% larger than a full stop on this page, yielded DNA microdots.

Primers designed to amplify the secret-message DNA were used to perform PCR directly on DNA microdots, without prior DNA solubilization[3], and the products were analysed by gel electrophoresis (Fig. 1c). An unamplified sample containing secret-message DNA yielded only a faint continuous smear (Fig. 1c, lane 2). In contrast, amplification of DNA microdots containing either 100, 10 or 1 copies of the secret-message DNA per haploid genome (lanes 3–5) each yielded a single product of the expected size (arrow). No such product was

detected using microdots containing either 0.1 (lane 6) or 0 (lane 7) copies per haploid genome, indicating a detection limit of about one secret-message DNA strand per haploid human genome. The amplified band in lane 4 of Fig. 1c (arrow) was excised, subcloned and sequenced. Use of the encryption key (Fig. 1b) to decode the resultant DNA sequence (Fig. 1d) yielded the encoded text, containing probably the most significant secret of the original microdot era: "June 6 invasion: Normandy" (Fig. 1d).

In preliminary experiments, microdots containing 100 copies of secret-message DNA per human haploid genome which had been attached using common adhesives to full stops in a printed letter, and posted through the US mail, yielded the correct PCR amplification product (data not shown). Our technique could therefore be used in a similar way to the original microdots: to enclose a secret message in an innocuous letter.

It should be possible to scale up the encoded message from the size of our simple example, perhaps by encoding a longer message in several smaller DNA strands. It should also be possible to use smaller microdots, which could be used for a variety of purposes, including cryptography and specific tagging of items of interest.

Catherine Taylor Clelland, Viviana Risca*, Carter Bancroft

Department of Physiology and Biophysics, Mount Sinai School of Medicine, New York, New York 10029, USA

e-mail: cbancro@smtplink.mssm.edu

**Present address: Paul D. Schreiber High School, Port Washington, New York 11050, USA*

1. Kahn, D. *The Codebreakers* (Scribner, New York, 1996).
2. Hoover, J. E. *Reader's Digest* **48,** 1–6 (April 1946).
3. Clayton, P. T. *et al. Arch. Dis. Child* **79,** 109–115 (1998).

Supplementary information is available on *Nature*'s World-Wide Web site (http://www.nature.com) or as paper copy from the London editorial office of *Nature*.

Neurochemicals aid bee nestmate recognition

The theory of kin selection[1], which revolutionized the study of social behaviour, requires the discrimination of relatives from non-relatives. Many animals possess this ability, but the underlying neurobiological mechanisms have not been studied. Here we provide evidence for the neurochemical modulation of nestmate recognition: treatment with octopamine agonists improves the discrimination of related nestmates from unrelated non-nestmates in honeybees.

We used a modification of a laboratory assay[2] that measures the probability that a group of five-day-old, laboratory-reared adult worker honeybees (*Apis mellifera*) will show aggression towards an introduced bee that is either a nestmate (from the group's natal colony) or a non-nestmate (from an unrelated colony). Group size was reduced from ten to three bees to make it possible for a single experimenter to inject all group members within a short period. Because the effects of octopamine injection are short-lived (about 60 min)[3], we treated bees with more persistent octopamine agonists: either 2,3-xylylaminomethyl-2′-imidazoline (XAMI)[4] or *N*′-(4-chloro-*o*-tolyl)-*N*-methylformamidine (DCDM)[5].

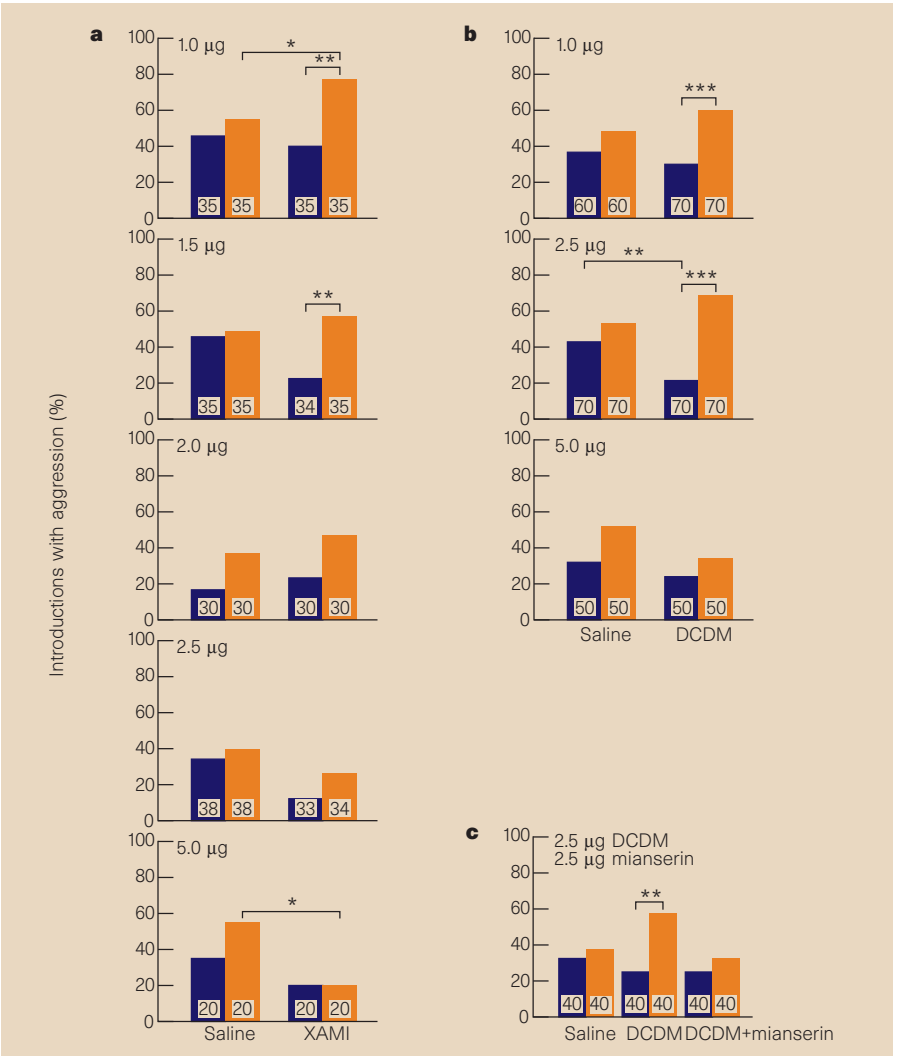

Figure 1 Effect of octopamine agonists on nestmate recognition in honeybees: **a,** XAMI; **b,** DCDM; **c,** DCDM plus mianserin (an octopamine antagonist). *P*-values are derived from two-way *G*-tests: **P*<<0.05; ***P*<0.01; ****P*<0.001. The number of introductions in each experiment is given in each bar. Purple bars, nestmate; orange bars, non-nestmate.

Bees given abdominal injections of 1.0 or 1.5 µg XAMI were significantly more likely to react aggressively towards non-nestmates than towards nestmates, but bees injected with saline were not (Fig. 1a). Comparisons with saline-injected bees suggest that the effect of XAMI was the aggregate result of two trends: decreased aggression towards nestmates and increased aggression towards non-nestmates. Only in one case was a trend significant by itself (aggression towards non-nestmates, with a dose of 1.0 µg; this was significant only at the $\alpha = 0.05$ level, and many statistical tests were performed). Higher doses of XAMI (2.5 and 5.0 µg) did not influence nestmate recognition but did cause a significant transient impairment of locomotor activity (data not shown), which might have interfered with the expression of aggressive behaviour. These results are consistent with depressed responses to both nestmates and non-nestmates in bees treated with the two higher doses (Fig. 1a). Octopaminergic agonists have been shown to have an effect on locomotion in other species[6].

To determine whether the results with XAMI reflected an octopaminergic process, we tested DCDM, an octopamine agonist from a different chemical family to XAMI. Results with DCDM were very similar to those with XAMI (Fig. 1b). Another indication of the specificity of the recognition effect is that it was eliminated when bees were treated with both DCDM and

(Fig. 1a) but Na_2CO_3–C diamond nucleation was not established under similar conditions. At a temperature as low as 1,150 °C for 120 hours, there was spontaneous nucleation of diamond octahedra of up to 4 μm and growth on seeds.

In the K_2CO_3–C system, diamonds grew on the seed crystals between 1,300 and 1,420 °C, but there was no nucleation. For the K_2CO_3 + C–O–H fluid + C system, after 20 and 40 hours at 1,250–1,420 °C, we also observed growth on seeds but without nucleation. However, runs of 120 hours at 1,150 °C, in the case of Na_2CO_3 with fluid as well, led to spontaneous diamond nucleation and growth on seeds (Fig. 1b). In all experiments in which fluid was added, we found metastable graphite in the form of small crystals. X-ray diffraction analysis did not reveal any decomposition of carbonates.

Diamond nucleation in the alkaline carbonate–graphite and alkaline carbonate-fluid–graphite systems, at the pressure and temperature studied, is largely determined by kinetics and takes place only in runs lasting tens of hours. The period of induction preceding diamond nucleation and growth increases as the temperature is decreased. This is the main difference between diamond synthesis in carbonate and metal melts.

Taking into account the influence of kinetics on diamond-forming processes, the established nucleation and growth temperature of 1,150 °C can hardly be supposed to be minimal, as it is lower than in the metal–graphite systems[6]. Catalytic activity in the system decreases in the sequence Na_2CO_3 + C–O–H fluid + C > K_2CO_3 + C–O–H fluid + C >> Na_2CO_3–C > K_2CO_3–C. Diamond growth rates vary in the range 0.01–4 μm h^{-1}, depending on the temperature and composition of the crystallization medium. In the 'dry' melt of Na_2CO_3, diamond crystallizes in the form of cubo-octahedra, and octahedra are formed in alkaline carbonate fluid-melts, which are most typical for natural diamonds.

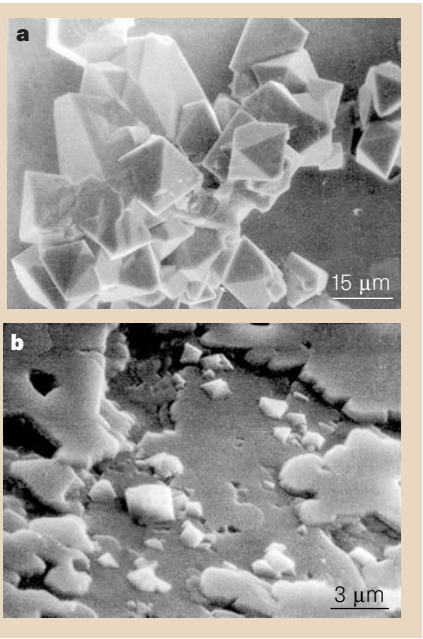

Figure 1 Scanning electron micrographs of diamonds. **a,** Octahedral diamonds (run NF-2). **b,** Diamond growth layers and spontaneous diamonds on {111} face of seed crystal (run KF-3).

Alkaline carbonate-fluid melts approximate the composition of a diamond-producing mantle environment[7–9]. Considering the abundance of carbonates in diamond-bearing rocks of magmatic[1] and metamorphic[10] origin, as well as the aqueous carbonaceous composition of mantle fluid[7], we suggest that alkaline carbonate-fluid melts represent the most likely medium for natural diamond formation.

Yu. N. Pal'yanov, A. G. Sokol, Yu. M. Borzdov, A. F. Khokhryakov, N. V. Sobolev

Institute of Mineralogy and Petrography, Siberian Branch of Russian Academy of Sciences, Novosibirsk 630090, Russian Federation
e-mail: palyanov@uiggm.nsc.ru

1. Haggerty, S. E. *Nature* **320,** 34–38 (1986).
2. Akaishi, S., Kanda, H. & Yamaoka, S. *J. Cryst. Growth* **104,** 578–581 (1990).
3. Arima, M., Nakayama, K., Akaishi, M., Yamaoka, S. & Kanda, H. *Geology* **21,** 968–970 (1993).
4. Taniguchi, T., Dobson, D., Jones, A. P., Rabe, R. & Milledge, H. J. *J. Mater. Res.* **10,** 2622–2632 (1996).
5. Pal'yanov, Yu. N. *et al. Russ. Geol. Geophys.* **5,** 920–945 (1997).
6. Wentorf, R. H. *Adv. High-Press. Res.* **4,** 249–281 (1974).
7. Schrauder, M. & Navon, O. *Geochim. Cosmochim. Acta* **58,** 761–771 (1994).
8. Harlow, G. E. *Am. Mineral.* **82,** 259–269 (1997).
9. Dawson, J. B. *Nature* **195,** 1075–1076 (1962).
10. Sobolev, N. V. & Shatsky, V. S. *Nature* **343,** 742–746 (1990).

Table 1 **Experimental results at 5.7 GPa**

Number	Temperature (°C)	Time (h)	Nucleation of diamond	Growth on seeds	Thickness of diamond layer (μm) {100} face	{111} face
Na_2CO_3 + graphite						
N-1	1,420	20	No	Yes	4	3
N-2	1,420	30	S (5 μm)	Yes	18	20
N-3	1,420	40	S (40 μm)	Yes	40	35
N-3	1,360	40	No	Yes	20	6
N-5	1,360	40	No	Yes	12	10
N-6	1,360	40	No	No	–	–
K_2CO_3 + graphite						
K-1	1,420	30	No	Yes	10	1
K-2	1,420	40	No	Yes	15	3
K-3	1,300	40	No	Yes	8	2
K-4	1,250	40	No	No	–	–
Na_2CO_3 + $H_2C_2O_4.2H_2O$ + graphite						
NF-1	1,420	20	S (13 μm)	Yes	20	14
NF-2	1,360	40	S (65 μm)	Yes	60	45
NF-3	1,250	40	No	Yes	10	8
NF-4	1,150	120	S (4 μm)	Yes	3	1.5
K_2CO_3 + $H_2C_2O_4.2H_2O$ + graphite						
KF-1	1,420	20	No	Yes	~1	~1
KF-2	1,250	40	No	Yes	25	4
KF-3	1,150	120	S (2 μm)	Yes	1.5	1

S, spontaneous nucleation; the size of newly crystallized diamonds is shown in parentheses.

Ageing, fitness and neurocognitive function

In the ageing process, neural areas[1,2] and cognitive processes[3,4] do not degrade uniformly. Executive control processes and the prefrontal and frontal brain regions that support them show large and disproportionate changes with age. Studies of adult animals indicate that metabolic[5] and neurochemical[6] functions improve with aerobic fitness. We therefore investigated whether greater aerobic fitness in adults would result in selective improvements in executive control processes, such as planning, scheduling, inhibition and working memory. Over a period of six months, we studied 124 previously sedentary adults, 60 to 75 years old, who were randomly assigned to either aerobic (walking) or anaerobic (stretching and toning) exercise. We found that those who received aerobic training showed substantial improvements in performance on tasks requiring executive control compared with anaerobically trained subjects.

Each of the 124 subjects was given a cardiorespiratory fitness test, in which the rate of oxygen consumption was measured, and a variety of cognitive tasks, including task switching[7], response compatibility[8] and stopping[9]. These tasks were chosen because a subset of their conditions require executive control processes and they have been shown through human lesion, neuroimaging and animal studies to be supported by frontal or prefrontal regions of the brain.

Task switching is a measure of the 'cost' of switching between tasks, indicated by the difference in reaction time between those trials in which subjects switch between tasks and those in which they continue to perform the same task; response compatibility

is a measure of the ability to ignore task-irrelevant stimuli, indicated by the difference between reaction time on response-compatible and response-incompatible trials; and stopping is a measure of the ability to abort a preprogrammed action, indicated by the reaction time to stop an action after a 'stop signal'.

Performance in other conditions on these same tasks, such as reaction time in the non-switch trials in the task-switching test, in the compatible trials on the response-compatibility task, and simple reaction time in the stopping test, depend less on executive control processes and so would not be expected to benefit from improvements in aerobic fitness.

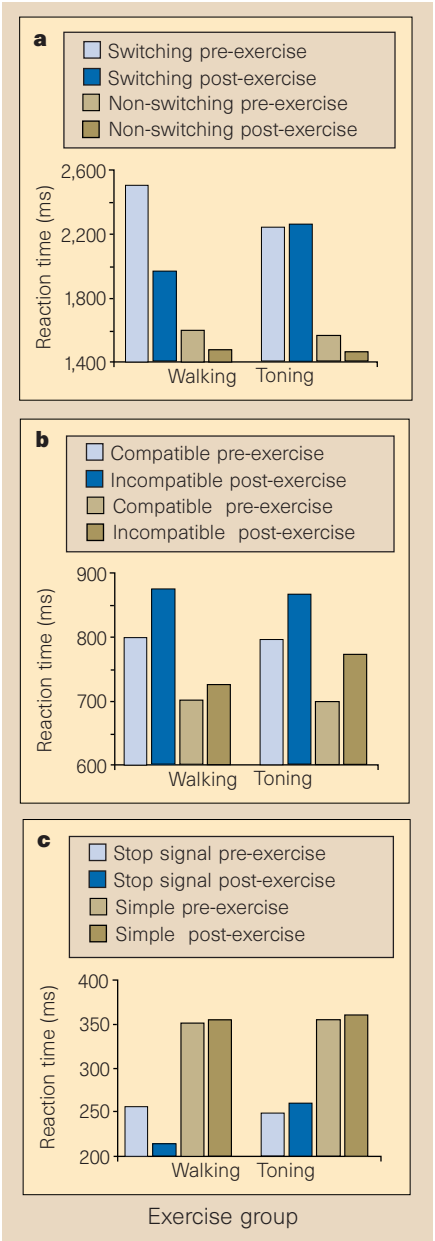

Figure 1 Tasks predicted to show selective improvements in performance for the walking but not for the toning group. **a,** Task switching; **b,** response compatibility; **c,** stopping. Experimental details are available from the authors.

Subjects in the walking group showed a significant improvement in the maximum rate of oxygen consumption (5.1%) compared with the toning group (−2.8%) after exercise training; the two groups displayed equivalent scores before exercise training.

Consistent with our 'selective improvement' hypothesis, performance improved significantly for subjects in the aerobic but not the toning group for task conditions depending on executive control processes (Fig. 1). In the task-switching test, subjects in the walking but not the toning group became much faster at switching between tasks following fitness training. Performance on the non-switch trials was equivalent for the walking and toning groups. In the response-compatibility test, the distractor-interference effect (difference between incompatible and compatible reaction times) decreased for the aerobic but not for the toning group, but there was no difference between groups on the compatible trials. In the stopping test, the reaction time for stopping was reduced for the aerobic but not for the toning subjects, whereas simple reaction time was the same for the two groups.

The three measures that were dependent on executive control processes and the integrity of the prefrontal and frontal cortex were all sensitive to the exercise intervention. However, the beneficial effect of aerobic exercise was selective: it did not affect performance on other measures in the same tasks that were not tied to frontally mediated executive functions.

The selective nature of the improvements produced by aerobic exercise, which affect only executive control processes supported by frontal and prefrontal regions of the brain, might explain the ambiguity of previous studies[10] relating aerobic fitness with improved neurocognitive function. The improvement we find requires only small increases in aerobic fitness.

Arthur F. Kramer*, Sowon Hahn*, Neal J. Cohen*, Marie T. Banich*, Edward McAuley*, Catherine R. Harrison*, Julie Chason*, Eli Vakil†, Lynn Bardell*, Richard A. Boileau*, Angela Colcombe*

**Beckman Institute, University of Illinois at Urbana-Champaign, 405 North Mathews Avenue, Urbana, Illinois 61801, USA*
e-mail: akramer@s.psych.uiuc.edu
†Department of Psychology, Bar-Ilan University, Ramat-Gan, Israel

1. Coffey, C. E. *et al. Neurology* **42,** 527–536 (1992).
2. Azari, N. P. *et al. Brain Res.* **552,** 279–290 (1992).
3. West, R. L. *Psychol. Bull.* **120,** 272–290 (1996).
4. Kramer, A. F., Larish, J. F., Weber, T. A. & Bardell, L. in *Attention and Performance* Vol. XVII (ed. Gopher, D. & Koriat, A.) (Academic, New York, 1999).
5. Black, J. E., Isaacs, K. R., Anderson, B. J., Alcantara, A. A. & Greenough, W. T. *Proc. Natl Acad. Sci. USA* **87,** 5568–5572 (1990).
6. Neeper, S. A., Gomez-Pinilla, F., Choi, J. & Cotman, C. *Nature* **373,** 109 (1995).
7. Rogers, R. D. *et al. Brain* **121,** 815–842 (1998).
8. Rafal, R., Gershberg, F., Egly, R. & Ivry, R. *Neuropsychologia* **34,** 1197–1202 (1996).
9. Hanes, D. P., Patterson, W. F. & Schall, J. D. *J. Neurophysiol.* **79,** 817–834 (1998).
10. Dustman, R. E., Emmerson, R. & Shearer, D. *J. Ageing Phys. Activ.* **2,** 143–181 (1994).

Developmental model for thalidomide action

Tabin has proposed a progress-zone model[1], based on published data, to explain the inhibition of limb morphogenesis by thalidomide. We do not think that his model convincingly explains the main features of thalidomide action.

We have previously listed[2] the factors that must be taken into account to explain the teratogenic action of thalidomide. First, the mechanism must be shown to occur in the embryo (preferably in a primate). Second, it must take into account the species specificity of thalidomide: it is teratogenic in all primates tested, has little effect in rabbits, and is not teratogenic in mice and rats. Third, thalidomide induces malformation of several organs but not of others, such as the brain. The heart, too, is an important target, and the many early postnatal deaths were probably due to cardiac malformation.

Any hypothesis on the teratogenicity of thalidomide should also be able to explain the defects induced in other organs by a common mechanism, which we believe cannot be inhibition of proliferation. It must also explain the sensitive period of thalidomide's action, which is confined to about two weeks in primates, although many induction and proliferation processes occur before and after this period. It needs to account for abnormal development but should not be too general because thalidomide has high specificity. The pattern of typical abnormalities cannot be mimicked by any other known teratogen, so its action must be unusual. Furthermore, thalidomide has many effects in different systems and dose levels, and few of these will be relevant to its teratogenic action.

With regard to Tabin's hypothesis[1], we must consider the fact that the critical period for thalidomide-induced typical limb malformations (amelia and phocomelia) is very early. According to investigations in primates[3,4], developmental stages 11 to 14 are affected, reaching (for example in the marmoset *Callithrix jacchus*) a maximum[5,6] at stages 11 to 12. Upper limb buds start to develop as early as stage 11. The apical ectodermal ridge (AER), which is critical according to Tabin's hypothesis, does not occur until stage 14, too late to bring about amelia or phocomelia.

We prefer an alternative explanation of

Biodiversity

Seed germination in rainforest fragments

Habitat loss and fragmentation remain the greatest threats to the world's biodiversity[1]. The local extinction of plant species from habitat fragments is common[2], although the reasons for this are not fully understood. Fragmentation is known to influence both birth- and death-related processes[3], but the disruption of plant reproduction, especially pollination and seed production, is thought to be particularly important[4,5]. The effects of fragmentation on post-pollination processes such as seed dispersal and germination have rarely been explored experimentally[6]. Here I show that seeds planted in forest fragments are less likely to germinate than those in continuous forest. This finding can have negative demographic consequences because it reduces the emergence of seedlings.

Heliconia acuminata is an Amazonian understorey herb that is found in both the experimentally isolated rainforest fragments and the continuous forest reserves of Brazil's Biological Dynamics of Forest Fragments Project. During the 1998 fruiting season, which lasted from March to May, I collected 1,668 seeds from more than 200 plants in continuous forest. I then distributed these seeds to seven forest fragments (four fragments of one hectare and three of ten hectares) and three continuous forest sites. Seeds from each maternal plant were distributed evenly across sites to avoid confounding potential maternal effects with fragmentation-related effects.

In each site, seeds were planted every 10 metres along five 100-metre transects. At each location on the transect, a seed was placed on the ground, placed in a plastic cup planted into the ground and filled with local soil (preventing removal of seeds by ants), and placed in a cup buried in the same way but covered with a fine mesh (to prevent all seed predation and accumulation of leaf litter). Seeds were checked each month to see whether they had germinated. One year after planting, I compared the proportion of emerging seedlings in each treatment in each site by using two-way analysis of variance (ANOVA)[7].

Seeds planted in continuous forest were between three and seven times more likely to germinate than those in forest fragments ($P < 0.0001$; Fig. 1). Seeds in fragments suffered from a variety of edge effects, including hotter, drier conditions and increased light penetration[8,9], all of which can affect the cues required for germination. I also found that seeds protected with mesh from leaf-litter accumulation and seed predation were more likely to germinate (although not significantly so), with the improvement being more marked in fragments than in forest sites (2.4- to 4.2-fold compared with 1.8- to 1.9-fold; Fig. 1). This asymmetrical improvement indicates that the greater accumulation of leaf litter in fragments (resulting from slower decomposition[8]) could be partly responsible for preventing germination as seeds become buried. Higher seed predation in fragments is an unlikely explanation, as predation is extremely low in all sites (E.M.B., unpublished data) and germination rates were similar for seeds placed on the ground and protected from predation in plastic cups.

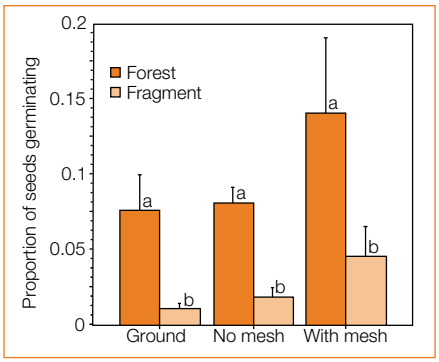

Figure 1 Mean proportion (± s.e.m.) of seeds germinating in continuous forest and fragmented sites in different experimental treatments. Differences in the proportion germinating in each habitat and treatment were assessed by ANOVA. The square root of the percentage germinating in each plot was arcsine-transformed, and habitat type and treatment were treated as fixed effects. The effect of habitat type was highly significant ($F_{1,24} = 22.623$, $P < 0.0001$), but that of planting treatment was not ($F_{2,24} = 2.336$, $P = 0.118$). The planting treatment × habitat type interaction term was also nonsignificant ($F_{2,24} = 0.028$, $P = 0.973$). Bars with different letters are significantly different from each other.

The results could be explained by the adaptation of seeds to conditions in the area from which they were collected, with seeds failing to germinate in fragments because of a change in location, rather than as a direct result of fragmentation. However, this mechanism seems unlikely unless seeds are adapted to very broad conditions, such as 'continuous forest'. Seeds were collected from an area of more than 3.5 km^2, and one site of continuous forest was about 20 km from the collection area. When compared with other continuous forest sites, this site never had the lowest germination frequency for any treatment. Even if local adaptation were responsible for the observed pattern, the demographic consequences for *Heliconia* populations in these fragments would be the same. Populations in fragments have few flowering individuals (E.M.B. and W. J. Kress, unpublished data), so most seeds for these populations probably come from outside the fragments.

Seeds from tropical rainforest plants rarely survive in seed banks for more than a year because they are highly susceptible to fungal pathogens, seed predation and burial under leaf litter[10]. My results therefore represent the outcome of a population's entire reproductive effort for a year. Although germination success is likely to vary from year to year, my results indicate that seeds dispersed into rainforest fragments are less likely to germinate than those in continuous forest.

Furthermore, my estimates of the effect of fragmentation on seed germination are probably conservative, as plants reproducing in forest fragments may be inbred and suffer from reduced heterozygosity[11]. If inbred seeds are less likely to germinate, these genetic effects could further reduce the recruitment of seedlings into forest fragment populations, helping to explain why plant populations in habitat fragments often fail to persist in the long term.

Emilio M. Bruna
Department of Environmental Science and Policy, and Center for Population Biology, University of California, Davis, California 95616, USA and Biological Dynamics of Forest Fragments Project, National Institute for Research in the Amazon (INPA), CP 478, Manaus AM 69011-970, Brazil
e-mail: embruna@ucdavis.edu

1. Wilcove, D. S., Rothstein, D., Dubow, J., Philips, A. & Losos, E. *Bioscience* **48,** 607–615 (1998).
2. Turner, I. M., Chua, K. S., Ong, J. S. Y., Soong, B. C. & Tan, H. T. W. *Conserv. Biol.* **10,** 1229–1244 (1995).
3. Jules, E. S. *Ecology* **79,** 1645–1656 (1998).
4. Bond, W. J. in *Extinction Rates* (eds Lawton, J. H. & May, R. M.) 131–146 (Oxford Univ. Press, New York, 1995).
5. Aizen, M. A. & Feinsinger, P. *Ecology* **75,** 330–351 (1994).
6. Wong, T. C. M., Sodhi, N. S. & Turner, I. M. *Biol. Conserv.* **85,** 97–104 (1998).
7. Sokal, R. R. & Rohlf, F. J. *Biometry* (Freeman, New York, 1995).
8. Didham, R. K. *Oecologia* **116,** 397–406 (1998).
9. Kapos, V., Wandelli, E., Camargo, J. L. & Ganade, G. in *Tropical Forest Remnants: Ecology, Management, and Conservation of Fragmented Communities* (eds Laurance, W. F. & Bierregaard, R. O. Jr) 33–44 (Univ. Chicago Press, 1997).
10. Vázquez-Yanes, C. & Orozco-Segovia, A. *Annu. Rev. Ecol. Syst.* **24,** 69–87 (1993).
11. Young, A., Boyle, T. & Brown, T. *Trends Ecol. Evol.* **11,** 413–418 (1996).

Vision

Dichromatism in macaque monkeys

Old World primates have trichromatic vision because they have three types of cone photoreceptor, each of which is maximally sensitive to short, middle or long wavelengths of light[1]. Although a proportion of human males (about 8% of caucasians, for example) have X-chromosome-linked colour-vision abnormalities[2], no non-human Old World primates have been found to be colour-vision defective[3,4]. We have tested 3,153 macaque monkeys but found only three dichromats, a frequency that is much lower than in humans.

Most defects in colour vision in humans arise from the loss of the gene that encodes

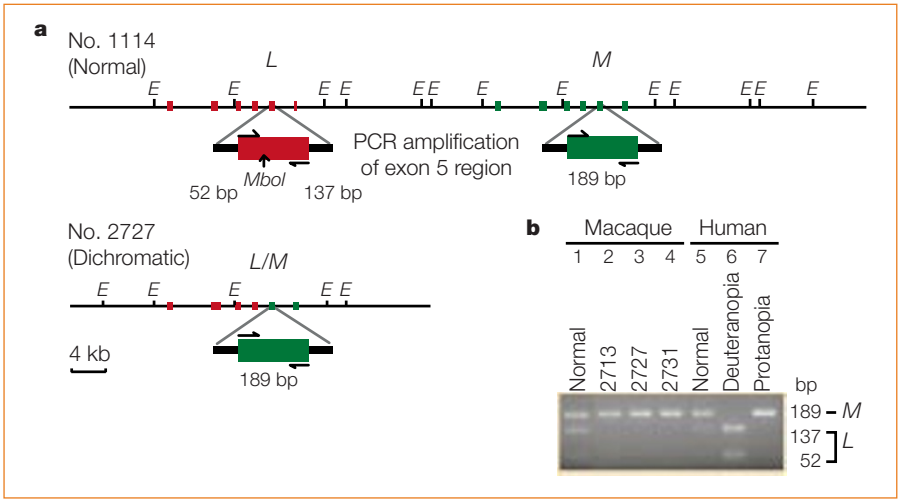

Figure 1 Physical maps of the *L* and the *M* genes. **a,** Top, the 77-kilobase (kb) region of a wild-type macaque (no. 1114), showing exons of the *L* (red) and *M* (green) genes. Enlarged exon-5 regions are shown underneath. The PCR primers and products for exon 5 of the *L* and *M* genes are shown in red (137 and 52 base pairs (bp), cleaved by *Mbo*I digestion) and green boxes (189 bp, uncleaved), respectively. An *Mbo*I site specific for exon 5 of the *L* gene is conserved among Old Word monkeys[8]. Bottom, the 36-kb region of a dichromatic candidate (no. 2727). The enlarged PCR-amplified fragment is shown underneath. **b,** Gel electrophoresis analysis. The bands of 189, 137 and 52 bp shown in **a** are indicated as *M* (green) or *L* (red). Lane 1, macaque wild type; lanes 2–4, subjects 2713, 2727 and 2731, respectively, showing only the exon 5 fragment of the *M* gene; lane 5, human wild type; lanes 6 and 7, deuteranopic (*M* cone absent) and protanopic (*L* cone absent) humans, respectively.

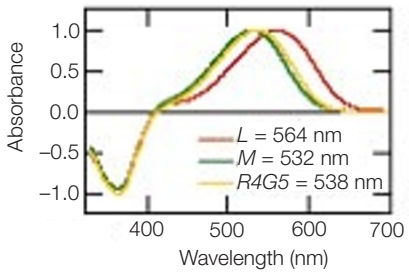

Figure 2 Absorbance spectra of *L*, *M* and hybrid (*R4G5*) pigments. Pigments expressed in 293T cells were extracted from the membrane fractions after 11-*cis*-retinal was added. Difference spectra were calculated from the spectra before and after photobleaching with light of wavelength ⩾590 nm for 1 min in the presence of 10 mM NH_2OH (ref. 13). The λ_{max} values of the *L* and *M* pigments are in good agreement with those previously measured by microscopic photometry[14].

pigments sensitive to either middle (*M*) or long (*L*) wavelengths of light. These genes are located on the X chromosome at Xq28 in a head-to-tail tandem array, and the repetitive units are gained or lost, and hybrid pigment genes generated, by unequal chromosomal recombination[5–7].

In our attempt to find dichromatic monkeys, we co-amplified the exon-5 region of the *L* and *M* genes with a set of common primers and discriminated between them with an *Mbo*I restriction site specific for the exon-5 fragment of the *L* gene[8] (Fig. 1a). We studied DNA from 744 male and 1,301 female crab-eating monkeys and 455 males and 653 females from 18 other macaque species, including samples from the Tsukuba Primate Center and the Nihon Monkey Center, and found only three DNA samples from males that lacked the exon-5 fragments of the *L* gene (Fig. 1b). These were from groups of crab-eating monkeys (26 males and 31 females) whose blood was sampled in the Pangandaran National Park, Indonesia.

The frequency of the dichromat males in this species (3 out of 744) is 0.4%, a value that is significantly lower (chi-squared test, $P < 0.002$) than in human males, for which a survey of 30,000 caucasian males found that 2% were dichromats[2]. No dichromat candidates were found in other macaque species.

We then constructed physical maps of the *L* and *M* genes from a wild-type (no. 1114) and a dichromatic (no. 2727) monkey from two genomic DNA libraries. The *L* and *M* genes were both present in the wild type but the dichromatic monkey had only a single pigment gene (Fig. 1a). Nucleotide sequence analysis then revealed that this single pigment gene was an *L*/*M* hybrid (called *R4G5*) consisting of exons 1 to 4 from *L* and exons 5 and 6 from *M*, indicating that the recombination point was located between exon 4 of *L* and exon 5 of *M*. Southern hybridization analysis revealed the presence of the *L*/*M* hybrid gene but no other *L* and *M* genes in this monkey. We found by polymerase chain reaction (PCR) using primers that specifically detect the *R4G5* hybrid gene that these three males and two females carried the hybrid gene.

We then used transient transfection into 293T cells to express complementary DNAs encoding the *M*, *L* and hybrid (*R4G5*) pigments (Fig. 2). Analysis of photobleaching difference absorption spectra showed that the absorbance maxima (λ_{max}) of reconstituted *L*, *M* and hybrid pigments are 564, 532 and 538 nm, respectively. The λ_{max} for the hybrid was red-shifted by 6 nm from that of the *M* pigment, indicating that these monkeys are almost protanopic (insensitive to red)[9,10].

In humans, between 58% and 78% of individuals possess several *M* genes[11,12], perhaps as a result of unequal recombination. In contrast, examination of 129 male crab-eating monkeys by quantitative Southern hybridization revealed that only six monkeys (5%) have more than one *M* gene, up to a maximum of four. All the other monkeys, apart from the dichromats, have just one *L* and one *M* gene. The variation in the number of *L* and *M* genes may be rare in macaques, but the sequence of the visual pigment genes is similar to that in humans[5,6].

Akishi Onishi*†, Satoshi Koike*‡, Miki Ida*‡, Hiroo Imai†, Yoshinori Shichida†, Osamu Takenaka§, Akitoshi Hanazawa||, Hidehiko Konatsu||, Akichika Mikami¶, Shunji Goto#, Bambang Suryobroto☆, Kenji Kitahara, Tetsuo Yamamori***

**Laboratory for Speciation Mechanisms I, National Institute for Basic Biology, 38 Myodaijicho, Okazaki 444-8585, Japan*
e-mail: yamamori@nibb.ac.jp
†Department of Biophysics, Graduate School of Science, Kyoto University, Kyoto 606-8502, Japan
‡Department of Microbiology and Immunology, Tokyo Metropolitan Institute for Neuroscience, Fuchu, Tokyo 183-8526, Japan
§Departments of Cellular and Molecular Biology and ¶Behavioural and Brain Sciences, and #Center for Applied Primatology and Human Evolutionary Modelling Research, Primate Research Institute, Kanrin, Inuyama, Aichi 484-8506, Japan
||Laboratory of Neural Control, National Institute for Physiological Sciences, Myodaijicho, Okazaki 444-8585, Japan
☆Department of Biology, Bogor Agricultural University, Jalan Pajajaran, 16143 Bogor, Indonesia
***Department of Ophthalmology, Jikei University School of Medicine, Minatoku, Tokyo 105-0003, Japan*

1. Tovée, M. J. *Trends Neurosci.* **17,** 30–37 (1994).
2. Fletcher, R. & Voke, J. *Defective Colour Vision: Fundamentals, Diagnosis and Management* (Hilger, Bristol, 1985).
3. Jacobs, G. H. & Harwerth, R. S. *Am. J. Primatol.* **18,** 35–44 (1989).
4. Jacobs, G. H. & Deegan, J. F. *Vis. Neurosci.* **14,** 921–928 (1997).
5. Nathans, J., Thomas, D. & Hogness, D. S. *Science* **232,** 193–202 (1986).
6. Vollrath, D., Nathans, J. & Davis, R. W. *Science* **240,** 1669–1672 (1988).
7. Deeb, S. S. *et al. Am. J. Hum. Genet.* **51,** 687–700 (1992).
8. Dulai, K. S. *et al. Vision Res.* **34,** 2483–2491 (1994).
9. Merbs, S. L. & Nathans, J. *Science* **258,** 464–466 (1992).
10. Neitz, J., Neitz, M. & Kainz, P. N. *Science* **274,** 801–804 (1996).
11. Drummond-Borg, N., Deeb, S. S. & Motulsky, A. G. *Proc. Natl Acad. Sci. USA* **86,** 983–987 (1989).
12. Jorgense, A. L., Deeb, S. S. & Motulsky, A. G. *Proc. Natl Acad. Sci. USA* **87,** 6512–6516 (1990).
13. Kojima, D. *et al. Biochemistry* **35,** 2625–2629 (1996).
14. Bowmaker, J. K., Dartnall, H. J. & Mollon, J. D. *J. Physiol. (Lond.)* **298,** 131–148 (1980).

Parasitoid behaviour and *Bt* plants

Transgenic crops that express genes targeted against insect pests may also affect non-target insects. For example, lacewings[1] and monarch butterflies[2] have been reported to be susceptible to toxins from *Bacillus thuringiensis* (*Bt*) that are expressed in *Bt* transgenic plants, although these results were obtained in small-scale laboratory assays in which insects were exposed to high levels of transgenically expressed toxin in no-choice tests. We show here that the behaviour of non-target insects can also play a part in determining how their populations will be affected by *Bt* plants.

Behaviour often influences the exposure of organisms to xenobiotics, and it is likely to be important for natural enemies of insect herbivores, whose primary route of exposure to engineered toxins will be through contact with hosts or prey feeding on plant tissues[3]. We have investigated this for a model system involving *Bt* oilseed rape (cv. Oscar, line O52) expressing the Cry1Ac toxin (which is highly active against many lepidopteran pests)[4], the diamondback moth (*Plutella xylostella*) and the parasitic wasp *Cotesia plutellae*. The wasp is a solitary endoparasitoid and an important enemy of *P. xylostella*[5], itself notorious as the first insect pest to evolve resistance to microbial *Bt* sprays in the field[6].

We find that, although parasitoid larvae forced to develop in *Bt*-treated susceptible moth larvae inevitably died with their hosts, behavioural factors are likely to limit the scale of this effect under field conditions. Furthermore, wasp parasitoids that had attacked *Bt*-resistant moth larvae on transgenic plants suffered no measurable adverse effects of *Bt* toxins on their behaviour as adults or on the survival of their larvae.

We investigated the performance of parasitoids against *Bt*-susceptible *P. xylostella* larvae by presenting them with young host larvae fed on transgenic (*Bt*) or wild-type oilseed rape for 4 h in 9-cm Petri dishes. In this no-choice situation, parasitoids oviposited into *Bt*-treated hosts, but the parasitoid larvae failed to complete their development. This was hardly surprising, given that all host larvae, whether exposed to parasitoids or not, died within five days of feeding on *Bt* plants — shorter than the minimum of seven days required by *C. plutellae* after oviposition to emerge from their host. In contrast, a new generation of adult parasitoids developed from 63% of *Bt*-susceptible moth larvae feeding on wild-type oilseed rape.

When parasitoids oviposited in larvae of a highly *Bt*-resistant laboratory strain of diamondback moth (NO-QA, originally selected with microbial *Bt*[6]) under the same conditions, there was no significant difference in parasitoid survival in resistant hosts fed *Bt* or wild-type oilseed rape (54% and 56% parasitism, respectively; $P=0.868$). The presence of *Bt* toxin in resistant host larvae therefore had no direct effect on parasitoid survival, confirming previous results with microbial *Bt* formulations[7].

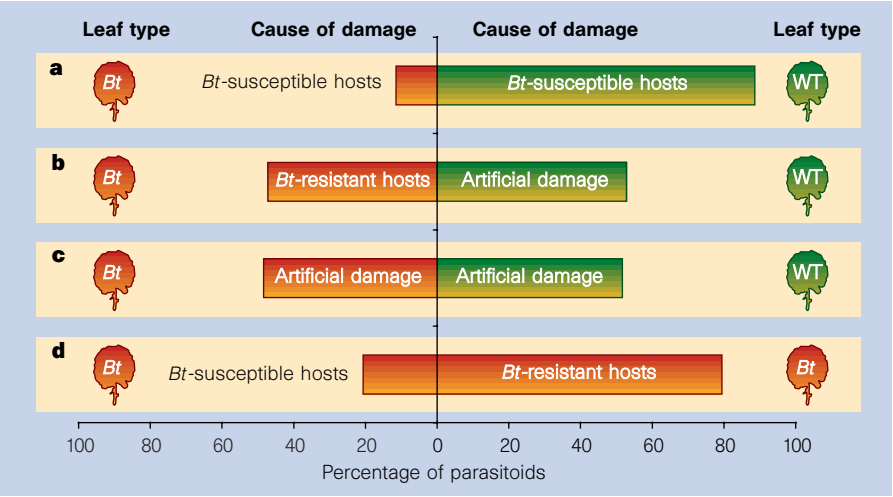

Figure 1 The percentage of parasitoids landing on *Bt* (brown) and wild-type (WT, green) oilseed rape leaves in choice tests in a wind tunnel. Parasitoids were released individually 70 cm downwind of two leaves placed 15 cm apart. Bars represent the percentage of parasitoids landing on each type of leaf. **a, b**, Host-damaged leaves were obtained by allowing two *Bt*-susceptible (**a**) or two *Bt*-resistant (**b**) diamondback moth larvae to feed on each leaf for at least 16 h. **c,** Leaves were artificially damaged by punching five 2-mm holes in each leaf. **d,** Attraction of parasitoids to *Bt* leaves damaged by either two *Bt*-resistant larvae or two *Bt*-susceptible larvae. About 40 parasitoid females were used for each bioassay.

Female parasitoids use herbivore-induced volatiles released from plants to locate their insect hosts, a behaviour that is critical for successful parasitism[8,9]. We used a wind-tunnel technique[10] to compare the flight response of the *C. plutellae* wasp towards *Bt* and wild-type leaves. For host-damaged leaves, *Bt*-susceptible or *Bt*-resistant *P. xylostella* larvae were allowed to feed on each type of leaf overnight. Flights were recorded as a choice if the wasp landed on a leaf within five minutes of take-off. The feeding damage inflicted by the hosts was measured after each bioassay.

The low consumption rate of *Bt* leaves by *Bt*-susceptible host larvae resulted in significantly ($P=0.005$) less feeding damage to the *Bt* leaves (mean, 9 mm^2) than to wild-type leaves (mean, 138 mm^2). When these leaves were placed in the wind tunnel, 89% of the parasitoids landed on the wild-type leaf and only 11% on the *Bt* leaf ($P<0.00001$) (Fig. 1a). No significant difference was found between feeding damage by resistant larvae on *Bt* and wild-type leaves ($P=0.33$), and the parasitoids did not distinguish between these two treatments ($P=0.43$) (Fig. 1b). Parasitoids did not prefer one plant type over the other if leaves were artificially damaged to the same degree ($P=0.50$) (Fig. 1c).

A further choice test compared *Bt* leaves damaged by either *Bt*-resistant hosts (feeding-damage mean, 101 mm^2) or *Bt*-susceptible hosts (2.6 mm^2; $P=0.0011$). In this test, 79% of the parasitoids flew to the *Bt* leaves damaged by resistant hosts, with only 21% choosing *Bt* leaves damaged by susceptible hosts, a difference that was highly significant ($P=0.00041$) (Fig. 1d).

Tactics aimed at suppressing pest populations risk disrupting the dynamics of their natural enemies by reducing host or prey density. These effects will be most pronounced for species (such as hymenopteran parasitoids) that tend towards greater ecological specialism and may even be specific to particular pest organisms.

Using *Bt*-resistant pests to evaluate direct effects of *Bt* toxins on parasitoid biology is a new way to assess ecotoxicological risk. The apparent lack of effect on the survival or host-seeking ability of the pest's enemy indicates that *Bt* plants may have an environmental advantage over broad-spectrum insecticides. The continued ability of *C. plutellae* to locate and parasitize *Bt*-resistant hosts on transgenic crops might even help to constrain the spread of genes for *Bt* resistance. Our results highlight the need to consider behavioural as well as toxicological aspects when looking at possible side-effects of transgenic crops on non-target organisms.

Tanja H. Schuler, Roel P. J. Potting, Ian Denholm, Guy M. Poppy
Institute of Arable Crops Research Rothamsted, Harpenden, Herts AL5 2JQ, UK
e-mail: guy.poppy@bbsrc.ac.uk

1. Hilbeck, A., Baumgartner, M., Fried, P. M. & Bigler, F. *Environ. Entomol.* **27,** 480–487 (1998).
2. Losey, J. E., Rayor, L. S. & Carter, M. E. *Nature* **399,** 214 (1999).
3. Schuler, T. H., Poppy, G. M., Kerry, B. R. & Denholm, I. *Trends Biotechnol.* **17,** 210–216 (1999).
4. Stewart, C. N. Jr *et al. Plant Physiol.* **112,** 115–120 (1996).
5. Talekar, N. S. & Shelton, A. M. *Annu. Rev. Entomol.* **38,** 275–301 (1993).
6. Tabashnik, B. E. *et al. Proc. Natl Acad. Sci. USA* **94,** 12780–12785 (1997).
7. Chilcutt, C. F. & Tabashnik, B. E. *Environ. Entomol.* **26,** 38–45 (1997).
8. Turlings, T. C. J., Tumlinson, J. H. & Lewis, W. J. *Science* **250,** 1251–1253 (1990).
9. De Moraes, C. M., Lewis, W. J., Paré, P. W., Alborn, H. T. & Tumlinson, J. H. *Nature* **393,** 570–573 (1998).
10. Du, Y. *et al. J. Chem. Ecol.* **22,** 1591–1606 (1996).

Prelude or requiem for the 'Mozart effect'?

Rauscher *et al.* reported that listening to ten minutes of Mozart's music increased the abstract reasoning ability of college students, as measured by IQ scores, by 8 or 9 points compared with listening to relaxation instructions or silence, respectively[1]. This startling finding became known as the 'Mozart effect', and has since been explored by several research groups. Here I use a meta-analysis to demonstrate that any cognitive enhancement is small and does not reflect any change in IQ or reasoning ability in general, but instead derives entirely from performance on one specific type of cognitive task and has a simple neuropsychological explanation.

Results from 16 studies on the effect of Mozart's music on the performance of cognitive tasks are summarized in Table 1. Meta-analysis[2] combining the effect sizes reported for all 20 published Mozart-to-silence comparisons (Table 1, top), involving a total of 714 subjects, yields an average cognitive enhancement of $d = 0.09$ standard deviations, or only 1.4 IQ points.

Most of the tasks listed can be classified as stressing either 'abstract reasoning' (Raven's Advanced Progressive Matrices, Stanford–Binet matrices, backwards digit span) or 'spatial–temporal processing'[3] (Paper Folding and Cutting, Revised Minnesota Paper Form Board). The Mozart effect for abstract reasoning is $d = -0.04$, whereas for spatial–temporal processing it is $d = 0.14$ (or 2.1 IQ points). Accordingly, exposure to ten minutes of Mozart's music does not seem to enhance general intelligence or reasoning, although it may exert a small improving effect on the ability to transform visual images.

However, this enhancement is essentially restricted to a single task, is one-quarter as large as that originally reported for a broader class of cognitive abilities, is not statistically significant (combined $Z = 1.14$, $P = 0.26$), and is smaller than the average variation of a single person's IQ-test performance (assuming a test reliability of 0.95, the 50% confidence interval would be 4.5 IQ points wide).

To account for the Mozart effect, Rauscher's group appealed to a model of cortical computation whose operations at the columnar level are compatible with qualities presumed to be present in Mozart's music and with the cognitive processing presumed to be involved in spatial–temporal tasks[1,3,4]. But any improvement in performance with music can also be explained by the fact that the complex visual transformation processes involved in three-dimensional mental rotation and similar difficult spatial tasks (such as paper folding and cutting) are associated with function of the right cerebral hemisphere[5], as is cognitive arousal[6,7].

In support of this, one study found that listening either to Mozart or to a passage from a Stephen King story enhanced subjects' performance in paper folding and cutting, but only for those who enjoyed what they heard[8]. Another experiment found that 8,120 British schoolchildren performed better in response to (presumably enjoyable) popular music than to Mozart's music, relative to a control group that heard a discussion of scientific experiments[9].

Mozart's effect on mood has been verified in standard questionnaires[10]. In a meta-analysis of eight comparisons (with 201 subjects) of auditory relaxation instructions with Mozart's music (Table 1, bottom), the music effect appears to be larger: $d = 0.20$ overall, and $d = 0.56$ for spatial–temporal processing. But as relaxation instructions aim to reduce arousal, it is not surprising that they should impair subsequent cognitive performance, especially on tasks that depend on the right hemisphere.

I conclude that a shared right-hemisphere locus provides a plausible explanation for an intermittent, small positive 'enjoyment arousal' effect of Mozart's music on difficult spatial tasks. It also explains the failure to find an effect from other stimulation, which may not be sufficiently enjoyable or arousing to subjects,

Table 1 **Studies of the effect of Mozart's music on the performance of cognitive tasks**

Task	*N*	*d*	*P*
Comparisons with silence			
Raven's Advanced Progressive Matrices[11]	78	−0.065	0.778
Raven's Advanced Progressive Matrices[12]*	20	0.00	1.000
Matrices (Stanford-Binet)[1,3]*	8	0.097	0.909
Matrices (Stanford-Binet)[13]*	12	−0.048	0.941
Matrices (Stanford-Binet)[14]*	16	−0.308	0.574
Backwards digit span[15]	24	0.149	0.730
Paper Folding and Cutting (Stanford-Binet)[1,3]*	8	1.389	0.140
Paper Folding and Cutting (Stanford-Binet)[16]	136	0.218	0.209
Paper Folding and Cutting (Stanford-Binet)[13]*	12	−0.356	0.586
Paper Folding and Cutting (Stanford-Binet)[14]	45	0.017	0.956
Paper Folding and Cutting (Stanford-Binet)[14]*	16	−0.989	0.085
Paper Folding and Cutting (Stanford-Binet elaborated)[4]*	53	0.724	0.013
Paper Folding and Cutting (Stanford-Binet elaborated)[17]*	38	−0.151	0.653
Paper Folding and Cutting (Stanford-Binet elaborated)[10]	86	0.057	0.795
Paper Folding and Cutting (Stanford-Binet elaborated)[14]	35	−0.011	0.975
Paper Folding and Cutting (computerized)[8]*	28	0.272	0.494
Revised Minnesota Paper Form Board[18]	51	0.082	0.775
Maze completion (paper-and-pencil)[19]*	14	0.000	1.000
Pattern Analysis (Stanford-Binet)[1,3]*	8	0.289	0.735
Short-term memory (character strings)[4]*	26	−0.072	0.861
Comparisons with auditory relaxation instructions			
Raven's Advanced Progressive Matrices[11]	77	−0.176	0.447
Matrices (Stanford-Binet)[1,3]*	8	0.000	1.000
Paper Folding and Cutting (Stanford-Binet)[1,3]*	8	1.622	0.094
Paper Folding and Cutting (Stanford-Binet elaborated)[14]	36	−0.032	0.925
Paper Folding and Cutting (Stanford-Binet elaborated)[20]*	8	0.489	0.571
Paper Folding and Cutting (Stanford-Binet elaborated)[21]*	32	0.814	0.033
Paper Folding and Cutting (Stanford-Binet elaborated)[22]*	24	0.867	0.054
Pattern Analysis (Stanford-Binet)[1,3]*	8	−0.685	0.434

N is the number of subjects in the comparison; *d* is the effect size measure, defined as the number of standard deviations by which the Mozart group performance mean is greater than the control group mean, based on the pooled variance of the two groups (performance for most tasks is measured by the number of test items correctly completed in a fixed time); and *P* is the two-tailed probability associated with affirming the null hypothesis (of $d = 0$). When effect sizes were combined in the meta-analysis, each was weighted by its associated degrees of freedom, or $N - 2$; when probabilities were combined, they were first converted to *Z*-values[2]. To be included, a study must have been published or submitted for publication, and had to compare the effects on the task of a Mozart composition (usually his sonata for two pianos, K.448) and either silence or auditory relaxation instructions, not different types of music or other non-musical auditory stimuli, any of which could be the source of the effect rather than Mozart[15]. To ensure that none of the measurements could have been contaminated by prior tasks or listening conditions, all comparisons are between two separate groups of adult human subjects, each performing the first cognitive task in a testing session, one listening to Mozart and the other to silence or relaxation instructions of equal duration beforehand.
*Extra information needed for these computations was obtained from the authors.